Laser Direct-Write of Nanoporous Optical Coatings: Preliminary Results

R. Ruizpalacios[1], H. Kyogoku[2], V. Sriram[1], K.L. Wood[1], and J.J. Beaman[1]

[1]Department of Mechanical Engineering, The University of Texas at Austin, Austin TX

[2]Department of Mechanical Engineering, Kinki University, Hiroshima, Japan

Abstract

The combination of nanoporous optical thin films prepared by the sol-gel process with direct-write capabilities has been an area of interest over the past decade. Recent advancements in both fields suggest the possibility of fabricating novel components for rapid prototyping purposes. This paper presents the work in progress done over the past year, initially aimed at process characterization. Standard silicate sol-gels were synthesized and deposited by spin coating on silicon wafers. Further post processing was done prior to laser densification with a CO_2 laser.

1. Introduction

The recent increase in demand for information bandwidth has created the need for improving current technologies for data, voice and video transmission. New technologies have emerged addressing different aspects of networking, such as transmission protocols, communication devices, and manufacturing methods of these devices. Transmission through optical fibers plays a fundamental role in the current and future infrastructure [1].

The current bottleneck in transmitting data optically does not lie in the long lengths of cabling required over large distances, but rather in delivering higher bandwidths to the end users in what has recently been named as ultra-high capacity optical networks. Two areas that address these needs include function integration in optoelectronic components and advanced materials, respectively. The combination of advanced materials derived from sol-gels with direct-write technologies, has the potential of addressing these initiatives. As documented in recent NSF and DARPA workshops, a critical area of research is the "Direct Writing" of components for industries such as telecommunications. Direct-write technologies are manufacturing processes characterized by the use of computer-generated patterns and shapes for direct fabrication without part-specific tooling. They represent a set of emerging technologies, competing with more conventional fabrication techniques primarily in the microelectronics field and lie at the forefront in research and development as alternatives of current photoresist technologies [2,3,4].

Sol-gel processing allows the creation of high optical-quality films and monoliths through the strict control of processing parameters (concentration, pH, temperature, humidity) in combination with high-purity sol-gel precursors [5]. This approach has received great attention because of the possibility of low processing temperatures and standard atmospheric conditions, and its ability to produce highly pure materials directly from their synthesis. Likewise, laser scanning has the ability to selectively achieve high-density levels of sol-gels comparable to vapor deposition and melting [6,7]. A direct relation exists between a sol-gel's density and index of refraction [8], hence the ability to control the index of refraction through density changes based on laser power control is an area of keen interest.

In this paper we report the work in progress done over the past year towards the development of a novel manufacturing process for the direct write of optical components, combining the advantages of controlled laser densification with sol-gel coating. The paper is organized as follows. First we present a description of the experimental procedures that were followed for preparation of the sol-gels, their deposition and heat treatment, followed by laser scanning. The following section presents the results and discussion in each of these areas.

2. Experimental Procedure

In this section we outline the experimental procedures that were followed, starting from the preparation of the sol-gel solution, the deposition of the solution by spin coating, the process for heat-treating the film, and the final laser densification step. Figure 1 illustrates in general the experimental procedure that was followed.
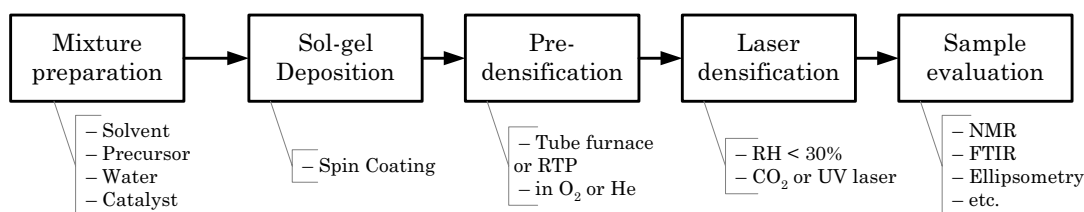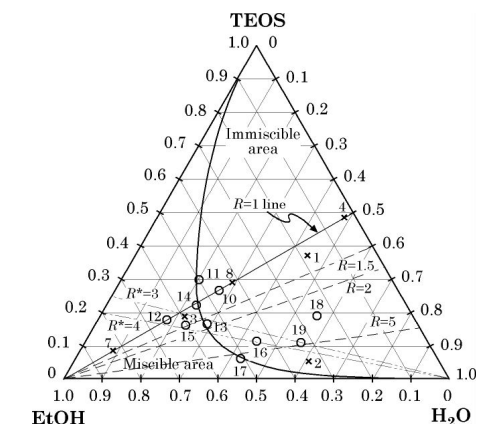

Figure 1. Outline of the experimental process

2.1 Sol-Gel Preparation

The sol-gel process consists, in general, in the hydrolysis of a precursor, in this case an alkoxide, in the presence of a catalyst (acid or base), and followed by condensation and poly-condensation reactions to form particulate or polymeric structures [5]. The solutions synthesized were based on well know purely inorganic silica-based systems [5,9,10,11].

For the preparation of the purely inorganic Si-based sol we used tetraethyl orthosilicate (TEOS) as the sol-gel precursor, ethanol as a solvent, de-ionized water, and hydrochloric acid as catalyst. A number of mixtures were prepared and are indicated in the ternary diagram of Figure 2(a), which is based on [5]. The preparation procedure, based on [9,10], consisted of a two-step hydrolysis process, followed by refluxing of the solution for 60 minutes at 60-65°C.

| Mixt. | Molar fraction (%) | | | R | R* | Density (g/cm^3) | Viscosity | |
	TEOS	H_2O	EtOH				Kinematic (cSt)	Dynamic (cP)
7	19.60	21.00	59.40	1.07	3.03	0.928	2.826	2.622
15	18.00	18.00	64.00	1.00	3.56	0.931	2.082	1.939
16	18.00	22.00	60.00	1.22	3.33	0.951	2.250	2.140
17	22.00	22.00	54.00	1.00	2.45	0.937	2.028	1.900
18	18.00	28.00	54.00	1.56	3.00	0.956	3.107	2.970
19	10.90	55.70	32.80	5.11	3.01	0.980	4.921	4.821

(a) Ternary diagram TEOS-EtOH-H_2O (b) Composition of mixtures

Figure 2. Molar ratios of various experiments

2.2 Deposition of Thin Films by Spin Coating

The films were spin coated on two types of substrates: Si (100) wafers, and borosilicate glass slides. Surface preparation is critical for successful deposition of the films. To achieve this, the substrates were cleaned with trichloroethylene, then rinsed with acetone, isopropyl alcohol, and de-ionized water using an ultrasonic bath. After this, the substrates were dried and stored in a drying cabinet, prior to deposition by spin coating.

The spin coating was carried out at various spinning velocities for various duration times under N_2 and standard air using a single-wafer spin processor. The spin-coating profiles consisted in an acceleration step, deposition of 20 µl of filtered solution, acceleration to desired speed, and finally a dwell period for solvent evaporation. Typical deposition velocities ranged from 2000 up to 5000 rpm, while the complete process time ranged from 40-60 sec.

2.3 Heat Treatment

Following the deposition step a consolidation or sintering step is required because of the highly porous nature of the as-spinned films. During sintering, an increase in density occurs due to further solvent and water evaporation (chemisorbed and physisorbed). So the initial chemistry and the desired final physical properties dictate the sintering or heat treatment temperature. The design of an appropriate heat treatment process represents a crucial step and a common roadblock for the achievement of films with thickness compatible with standard single-mode fiber optics. For this reason we devoted a substantial amount of time experimenting with various heating profiles, atmospheres, and processing equipment. A good understanding of the evolution of the psychochemical properties after the heat treatment step is required to characterize and ultimately control the process. With this in mind, we performed a series of experiments that involved the drying and densification of the films that would provide evidence and insight. The main issues explored were the relationship between heating temperature and thickness or index of refraction, and the effects of the drying step on the final structural composition of the film.

The films were heat-treated using a hot plate (120–200°C), a horizontal tube furnace (200–880°C), and an experimental vertical furnace (400–900°C) developed in our lab for rapid thermal annealing; all of them having controlled environment capabilities. Various dwell times and heating rates under He or O_2 gas flow were implemented.

2.4 Film Characterization: Techniques

For sample evaluation, process characterization, and process optimization, we used a number of standard techniques, which are described below.

For the analysis of the sol-gel solutions we used Nuclear Magnetic Resonance (NMR) spectroscopy for structure analysis. The viscosity was measured 24 hrs after preparation, with a Cannon-Frenske kinematic viscometer. Multiple-Angle Ellipsometry carried out in air was used for measurement of thickness and index of refraction. Fourier Transform Infrared Spectroscopy (FTIR) was used for evaluation of the molecular structure of the deposited films for various concentrations and heat treatment procedures. Atomic force microscopy (AFM) was employed to measure surface roughness and observe film morphology.
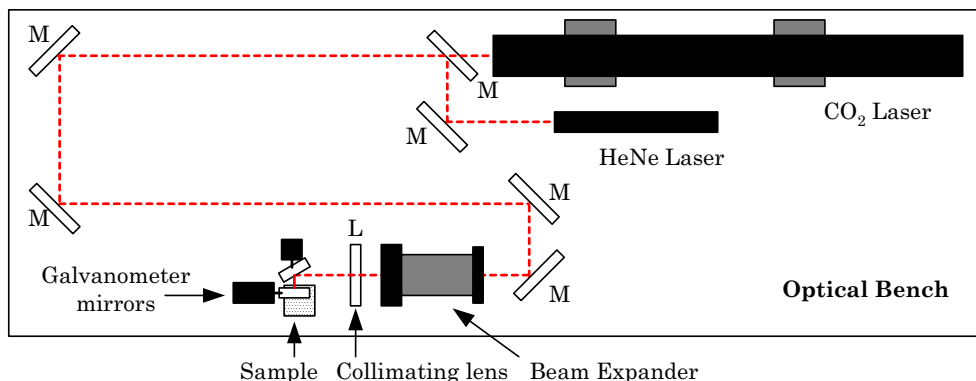
Figure 3. Schematic of optical setup for laser densification.

2.5   Laser Densification

Laser densification was performed with a CO_2 laser (λ=10.6μm), with maximum power of 50 W, beam diameter at exit of cavity of 3.5mm, and a spot size at the working surface of ~80μm. The control of laser power is performed by a pulse-width modulation (PWM) scheme. Both software and hardware versions were implemented, being the latest the most consistent one. Figure 3 shows a schematic of the optical assembly. A galvanometer-mirror assembly, which was controlled by a PC, deflected the beam onto the working surface, following the desired geometry. The position of the beam and the laser power were controlled simultaneously by a single graphical interface programmed in LabVIEW. The laser power was varied from 0.5–4.0 W, while scanning speeds from 0.486–2.429 cm/s, with a spot size of ~80μm ($1/e^2$). The purpose of the initial experimentation was to find an appropriate operating window for laser power and scan speed that would produce smooth tracks in a controllable manner.

3.   Results and Discussion

3.1   Effects of Composition on Structure, Physicochemical Properties and Morphology

Optical waveguides require a high degree of purity (typically <1 ppb of metallic compounds) and property uniformity, in combination with the desired index of refraction. For this reason, the election of both the sol-gel type and the synthesis procedure will dictate how well these requirements can be fulfilled. As mentioned before, we began by synthesizing a purely inorganic silicate sol-gel, which has been well documented in the literature [5, 9,10,11,12]. For this study, we made a number of sol-gel solutions, exploring various regions in the ternary diagram TEOS-H_2O-EtOH (Figure 2a). The compositions and properties of typical sol-gel solutions are given in the table of Fig. 2(b). The molar ratios between water to alkoxide, R, and solvent to alkoxide, R^*; are defined as: R=[H_2O]/[TEOS] and R^*=[EtOH]/[TEOS]. Different lines of constant R and R^* are indicated in the ternary diagram of Figure 2(a).

Si-NMR spectroscopy has been extensively employed to investigate the polymerization kinetics in the sol-gel process [5,13]. The NMR results of the typical sol-gel solutions are shown in Fig. 4. Fig. 4(a) shows a broad profile with no detectable peaks, which can be associated to a high degree of polymerization, as in a three-dimensional network structure. On the other hand, the spectrum from Fig. 4(b) with sharp peaks can be interpreted as a structure poorly branched., where the solutions presented low viscosity, and resulting in films prone to cracking.
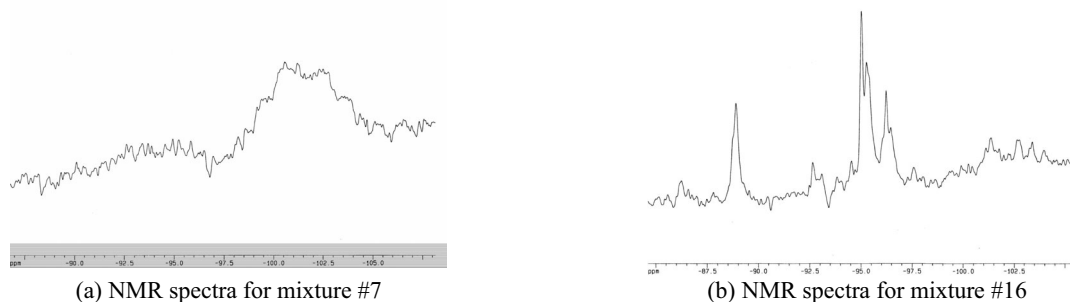
(a) NMR spectra for mixture #7   (b) NMR spectra for mixture #16

Figure 4. Typical plots from NMR and FTIR spectroscopy.

The water content on the sol affects greatly the structure and optical characteristics of the spin-coated films [15]. In particular, the index of refraction depends strongly on the water content remaining in the films. Therefore, we also evaluated the effects of the molar ratio R on the thickness and index of refraction. The combination of $R = 2$ and $R^* = 4$, produced $t_f = 652$ nm and $n = 1.4134$; while for $R = 5$ and $R^* = 4$, we observed a substantial increase of both properties to $t_f = 905$ nm and $n = 1.4401$. Although this is in agreement with the work done by Fardad [15], films with high R values cracked during sintering at temperatures above 400°C.

The morphology of the spin-coated films is influenced by both the composition of the solution and the spin-coating conditions. Solutions with high branching and mid- to high viscosity (~2.4 cP), produced smooth surfaces with an R_a on the order of 10 nm. On the other hand, less branched solutions produced cloudy and inhomogeneous films, with a higher tendency to crack.

3.2 Deposition of Single Layer Films

After studying the effects of the mixture composition, we explored the various processing parameters involved in the deposition of films, in this case by spin coating. Our goal was to characterize the process in order to control it and achieve repeatability. The homogeneity and thickness uniformity of spin-coated films strongly depend on the spin-coating speed and time, and also on the viscosity of the sol-gel solution, as observed from the following equation [16]:
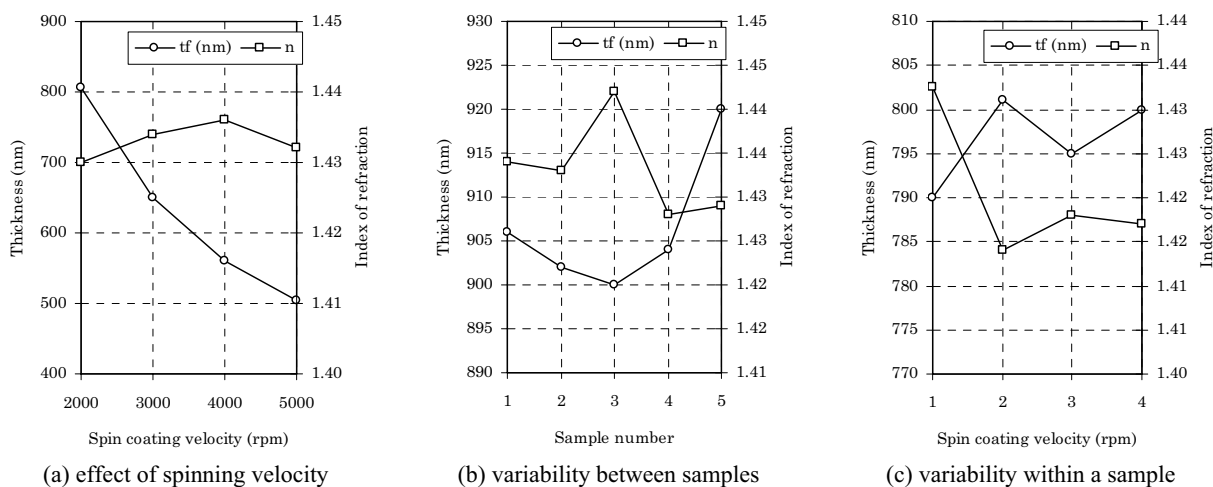

(a) effect of spinning velocity   (b) variability between samples   (c) variability within a sample

Figure 5. Various factors that affect the spin coating of films.

495

$$t_{final} = c_o \left(\frac{3\eta e}{2(1-c_o)\rho\omega^2} \right)^{\frac{1}{3}} \tag{1}$$

where c_o is the solids concentration, η the dynamic viscosity, e the evaporation rate (assumed constant), ω the angular velocity, and ρ the initial density.

Viscosity plays a fundamental role for proper deposition by spin coating. In our study we were able to verify this (see Fig. 2b). For viscosities greater than 2.5 cP we found good spinnability and repeatability. Although for a viscosity of 4.8 cP, cracking of the film took place during the heat treatment process, induced mainly by thermal stress effects. Viscosity in a sol-gel solution depends on many factors, and changes over time, reaching a maximum during gelation [5]. In our study we found that increasing the water content, for example at R values greater than 4, caused the viscosity of the sol-gel solutions to increase (see Fig. 2b). On the other hand, we found that too great of a water content was detrimental for further post processing, during heat treatment or subsequent layer deposition. We found that a spinning velocity of 4000 rpm, in combination with $R=3$ or 4 and $R^*=2$ produced consistent results. Further control of film thickness and index of refraction can be done by addition of solvent, in this case EtOH.
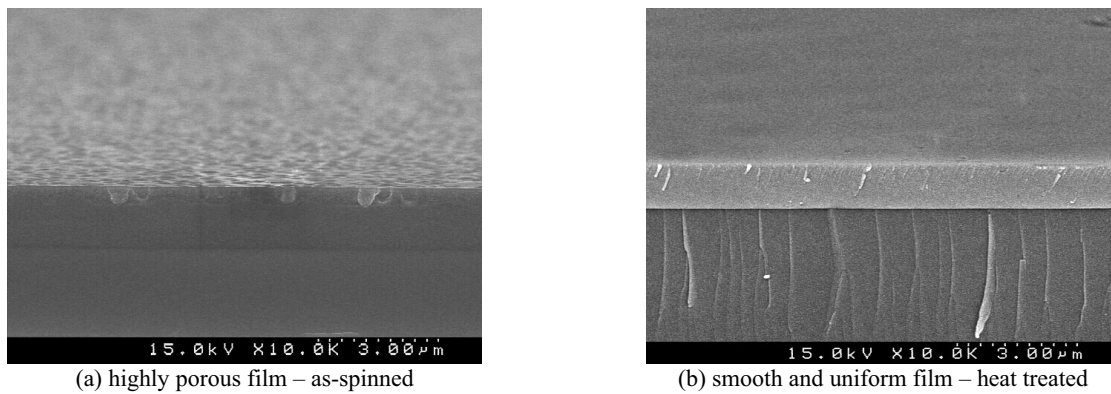
(a) highly porous film – as-spinned	(b) smooth and uniform film – heat treated

Figure 6. SEM pictures of porous and sintered films.

For process design, we were interested in studying the effects of spinning velocity, together with variability between samples and within a single sample. Figure 5(a) shows the effect of spinning velocity on the thickness and index of refraction of the as-spin-coated film. The thickness decreases with increasing spinning velocity. On the other hand, the index of refraction slightly increases with a spinning velocity of 4000 rpm. This result was in accordance to the equation proposed by Syms and Holmes [17], which states: $t_f = k\omega^{-\gamma}$; where k and γ are constants. Figure 5(b) shows an example of variability in thickness and index of refraction of samples coated with the same solution. The differences in thickness and index of refraction among the samples are about 20µm and 0.02, respectively, although the index of refraction is affected by the thickness. Figure 5(b) shows an example of unevenness in thickness and index of refraction in the same sample. The differences in thickness and index of refraction were observed to be in the order of 10 µm and 0.013, respectively.

3.3 Heat Treatment of Films

As mentioned above, the design of an appropriate heat treatment process is crucial for the fabrication of uniform crack-free films. This can be observed by comparing Figures 6(a) and (b),

where the highly porous nature of the as-spinned films is evident, while almost completely disappearing at high processing temperatures (~800°C). To determine the heat treatment profile, the TGA analysis was carried out (plot not shown). The change in weight took place at two stages: below 500 K and over 500 K. During the first stage, the rapid decrease in weight is mainly attributed to the evaporation of water and the volatilization of remaining ethanol. In the second stage, the gradual weight reduction is attributed to the combustion of organic compounds [14]. This result suggests sintering followed by viscous flow of the SiO_2 structure.

Further more, we studied the influence of a drying step at low temperature prior to baking at higher temperatures. This drying step was performed in a hot plate under He or O_2, with a temperature of 150°C for 15 minutes. After this, the samples were heated at a rate of 4°C/min until a certain temperature T_{max}, and held there for 20 min under O_2. Table 1 shows the various conditions, together with the values for thickness and index of refraction. FTIR transmission spectroscopy was employed to compare these samples, and the results are presented in Figure 7. From these plots we can make the following observations. The drying in O_2 results in no C-H bonds (ethyl group), which are found in the range of 1400-800 cm^{-1}, while on the rest of the samples they are still present. In samples heated at 400°C there is a broad band around 3400 cm^{-1} corresponding to O-H stretching in H_2O, which is evidence of remaining H_2O in the film. This shoulder almost completely disappears for samples heated at 880°C. This is desired for optical communications, since hydroxyl groups are generally associated with attenuation loss. In sample 4, it is also observed that there is no presence of SiC_6H_5, appearing around 667 cm^{-1}. Si-OH bonds are absent in samples heated to 880°C, irrespective of whether the sample was dried in O_2 or He. Peaks for the Si-O-Si bending mode appear at higher wavenumbers for samples heated at higher temperatures, which has been correlated to stress relief phenomena [18].

Table 1. Experimental conditions for studying the effects of a drying step.

Sample	T_{drying} (°C)	Drying Atmosphere	T_{max} (°C)	Baking Atmosphere	Thickness (nm)	Index of refraction
1	150	He	400	O_2	646.82	1.3920
2	150	He	880	O_2	495.34	1.4013
3	150	O_2	400	O_2	482.15	1.3899
4	150	O_2	880	O_2	495.09	1.4064
5	None	None	400	O_2	522.90	1.3933
6	None	None	880	O_2	500.00	1.4000

3.4   Laser Densification

In the case of sol-gel SiO_2 thin films on Si wafers, CO_2 laser is not absorbed well because of the small thickness of the films and the low absorption of Si at this wavelength. For this reason we changed the substrate to borosilicate glass slides. A continuous wave (CW) mode was used for the laser densification of the sol-gel films. We observed that it is critical to maintain a constant power within <5% in oder to obtain a continuous track at low energy densities. In many cases we observed a high degrees of cracking, perhaps caused by the uneven heating and cooling experienced by the film.
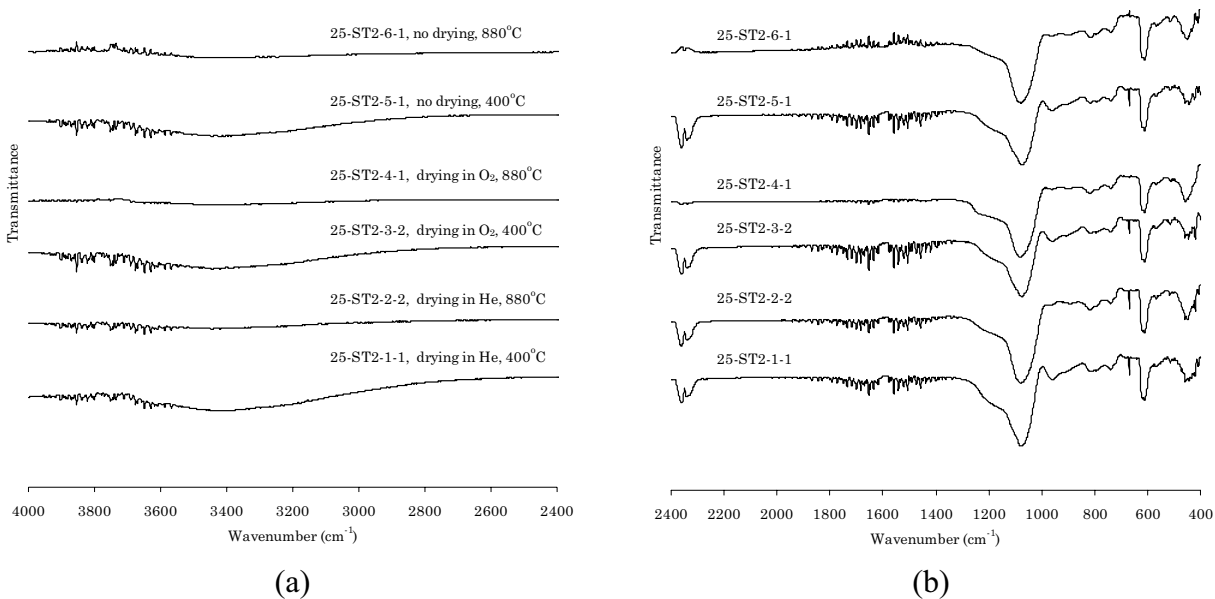
Figure 7. FTIR transmittance plot: influence of drying step.

Figures 8(a) and (b) show the changes in shape of the tracks with continuous laser power at the process time of 1.40 s and 0.65 s, respectively. In both cases, continuous tracks were obtained, but the track is smooth only at 0.93 W. Thus the morphology of the surface of the tracks is greatly affected by the laser power. In the case of the SiO_2 thin films on borosilicate glass, it is important for the laser power to keep less than 0.93 W to fabricate the continuous smooth tracks. For the CW mode, we observed a linear increase in the track width with increased laser power. Different scanning speeds produced a change in these slopes. As described above, since the range of laser power, in which the smooth tracks can be fabricated, is less than 0.93 W, it is necessary to examine the relation between the width and the laser power to control the width of waveguides accurately.

Figure 8(c) and (d) show SEM images of laser-densified tracks. Higher power and slower scanning speeds produced many defects, such as holes and bumps on the track. This phenomenon suggests that a closer examination of the heat-treatment process of deposited films is required to fabricate smooth convex-type tracks. For the energy density levels in our experiments, we observed concave tracks. This was the case for 0.93 W and a scanning speed of 1.458 cm/s. Defects such as bumps were still observed on both sides of the track, while the depth of the track was in the order of 10 nm. For these tracks the surface was very smooth, although the presence of cracks was observed at the boundary between the matrix and the heat-affected zone.
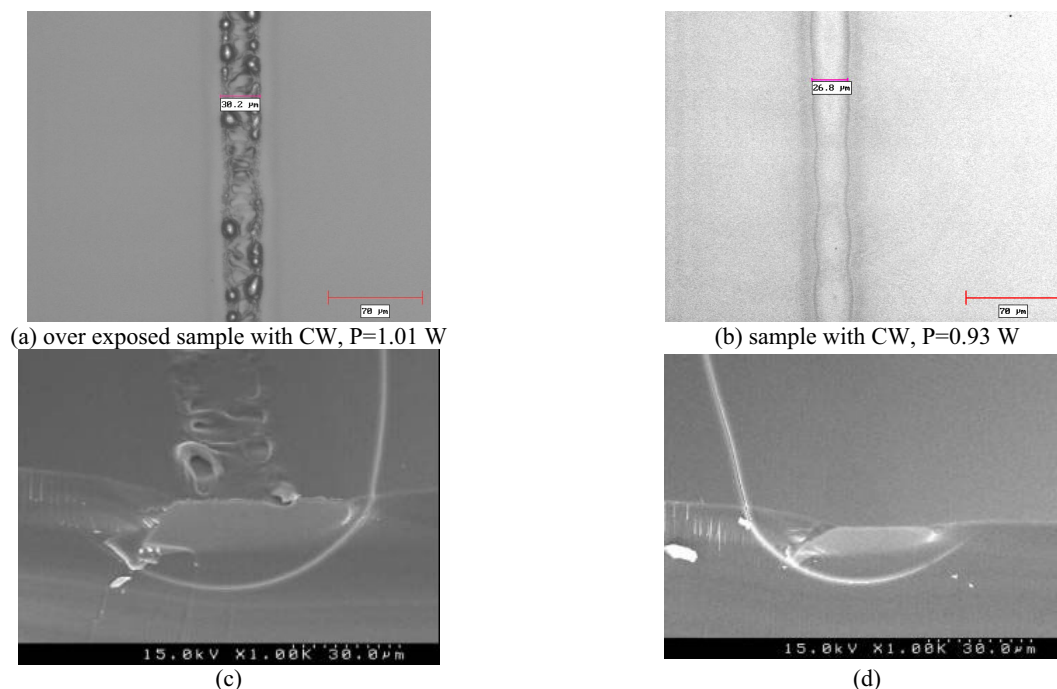
(a) over exposed sample with CW, P=1.01 W

(b) sample with CW, P=0.93 W

(c)

(d)

Figure 8. Images of laser densified sol-gel films.

4. Conclusions and Future Work

In this study we systematically investigated the materials design of sol-gel silica solutions, the fabrication conditions for the deposition of homogeneous thin films, and some initial experimentation with laser densification by a CO_2 laser. From our studies we concluded the following:

(1) For the successful deposition of purely inorganic silicate sol-gel by spin coating, the molar concentration of compounds plays a fundamental role since only a narrow combination of them can be applied. Specifically, the molar ratio of water to alkoxide precursor, R, has a strong effect in viscosity and structure.

(2) It was found that the uniformity of the spin-coated film strongly depends on the viscosity of the sol-gel solutions. The suitable film can be fabricated at the viscosity of more than 2.5 cP, but in the case of 4.8 cP, the cracking of the film took place by heating because of thermal stress. Viscosity also greatly affects the final thickness of the films.

(3) The heat treatment temperature strongly affects not only the thickness of the films but also their morphology and characteristics. The thickness of the films decreases with increasing heat treatment temperature, on the other hand, the index of refraction increases.

(4) The sol-gel films with high index of refraction could be fabricated by examining the contents of sol-gel solutions, the spin-coating conditions and the heat-treatment conditions in detail.

(5) The drying of the film at low temperature under oxygen, prior to sintering or laser densification, helps reduce undesired chemisorbed and physisorbed water and solvent from the film. Further analysis of this hypothesis is required, by measuring the attenuation loss in the films.

(6) We found that a small operating window between laser power and scanning speed exists for the fabrication of uniform and smooth tracks with a CW CO_2 laser. Further investigation is still required. A laser with smaller wavelength might help produce better results.

Acknowledgements

References

[1]   Hecht, J. (1999). *Understanding Fiber Optics*, 3rd edition, Prentice Hall, NJ.

[2]   Church, K. H., Fore, C., et al. (2000). "Commercial applications and review for direct write technologies." *Materials Development for Direct Write Technologies*, San Fco., CA, Materials Research Society.

[3]   Pique, A. and Chrisey, D.B. (ed), (2002), *Direct-Write Technologies for Rapid Prototyping Applications*, Academic Press, San Diego, CA.

[4]   Miura, K., J. Qiu, et al. (1997). "Photowritten optical waveguides in various glasses with ultrashort pulse laser." *Applied Physics Letters*, 71(23): 3329-3331.

[5]   Brinker, C.J., Scherer, G.W. (1990). *Sol-Gel Science*. San Diego, CA, Academic Press, Inc.

[6]   Shaw, D.J., King, T.A. (1990), "Densification of sol-gel silica glass by laser irradiation", SPIE 1328, *Sol-Gel Optics*, p 474-479.

[7]   Chia, T. (1992). "Laser Densification of Gel-Silica Glasses and Optical Application", Ph.D. Diss., University of Florida.

[8]   Hench, L. L. (1998). *Sol-Gel Silica*. Westwood, NJ, Noyes Publications.

[9]   Sakka, S., Kamiya, K., (1982), "The Sol-Gel Transition in The Hydrolysis of Metal Alkoxides in Relation to The Formation of Glass Fibers and Films", *Journal of Non-Crystalline Solids*, Vol.48, pp.31-46.

[10]   Sakka, S., Kamiya, K., Makita, K., Yamamoto, Y., (1984), "Formation of Sheets and Coating Films from Alkoxide Solutions", *ibid.*, Vol.63, pp. 223-235.

[11]   Righini, G., Pelli, S. (1997), "Sol-Gel Waveguides", *Journal of Sol-Gel Science and Technology*, 8, pp. 991-997.

[12]   Parrill, T.M. (1994), "Heat treatment of spun-on acid-catalyzed sol-gel silica films", *Journal of Materials Research*, Vol.9, No.3, pp.723-730

[13]   Brinker, C.J., et al (1984), "Sol-Gel transition in simple silicates II", *Journal of Non-Crystalline Solids*, Vol.63, (1984), pp.45-59.

[14]   Primeau, N., et al (1997) "The effect of thermal annealing on aerosol-gel deposited SiO_2 films: a FTIR deconvolution study", *Thin Solid Films*, 310, pp.47-56.

[15]   Fardad, M.A. et al (1995), "Effects of H_2O on Structure of Acid-Catalysed SiO2 Sol-Gel Films", *Journal of Non-Crystalline Solids*, Vol.183, pp.260-267.

[16]   Meyerhofer, D. (1978). "Characteristics of Resist Films Produced by Spinning." Journal of Applied Physics, 49(7), p 3993-3997.

[17]   Syms, R.R.A., Holmes, A.S., (1994), "Deposition of thick silica-titania sol-gel films on Si substrates", *Journal of Non-Crystalline Solids*, Vol.170, pp.223-233.

[18]   Ramkumar, K., Saxena, A.N. (1992) "Stress in SiO2 films deposited by plasma and ozone tetraethylorthosilicate chemical vapor deposition processes", *Journal of the Electrochemical Society*, Vol.139, pp.1437-1442.